PAPER

3D shape measurement of shiny surfaces based on optimized combination of fringe patterns of different intensity

IOP Publishing Measurement Science and Technology
Meas. Sci. Technol. **32** (2021) 035203 (7pp) https://doi.org/10.1088/1361-6501/abc49d

3D shape measurement of shiny surfaces based on optimized combination of fringe patterns of different intensity

Yifan Wei[1], Lei Lu[2], Jiangtao Xi[1], Yongkai Yin[3], Yanguang Yu[1], Jun Tong[1] and Qinghua Guo[1]

[1] School of Electrical Computer and Telecommunications Engineering, University of Wollongong, Wollongong, NSW, 2522, Australia
[2] College of Information Science and Engineering, Henan University of Technology, Zhengzhou 450001, People's Republic of China
[3] School of Information Science and Engineering, Shandong University, Jinan 250100, People's Republic of China

E-mail: lulei@haut.edu.cn

Received 29 February 2020, revised 11 October 2020
Accepted for publication 26 October 2020
Published 14 December 2020

Abstract

Image saturation is a challenging problem for three-dimensional shape measurement of objects with shiny surfaces using fringe projection profilometry technology. This paper presents a new method based on projection of multiple fringe patterns, providing an effective solution to the problem. First, a set of phase shifted sinusoidal fringe patterns with different intensity levels are projected to the object of interest, and the reflections are captured by the camera. With the captured images a set of masks are created, which are able to pick up the unsaturated data from the captured images. The unsaturated data are then combined based on maximal Signal-to-noise Ratio (SNR) scenario, and the combined images are used to retrieve the phase information. Comparing to existing methods, the proposed technique is advantageous by improved measurement accuracy due to the improved SNR. The performance of the proposed method is verified by the experiments.

Keywords: surface measurements, phase measurement, fringe analysis, phase shift

(Some figures may appear in colour only in the online journal)

1. Introduction

Phase shifting profilometry (PSP) is an effective method for non-contact three dimensional (3D) imaging and measurement [1–4] with a wide range of applications including industry, cultural heritage, medicine, etc. With PSP, sinusoidal fringe patterns are projected onto the object surface and deformed by the height of the object. The deformed fringe patterns are captured by a camera and then analyzed to reconstruct the profile of objects. However, a requirement limiting the application of PSP is the surface of object needs to be diffusive. In practice, this requirement cannot always be met as the surface may be dark or bright, rough or shiny, leading to distortion of the captured fringe patterns [5–7]. In the cases of shiny surfaces, reflection saturation can happen, resulting in significant errors in the extracted phase maps and consequently the 3D shape measurement [8].

Many approaches have been proposed to solve the light saturation problem. Chen *et al* [9] proposed an adaptive algorithm to avoid the saturation. The object is reconstructed with the maximum intensity at the first time, and then, the suitable intensity value for the saturation area is calculated by fitting a polynomial function. At last, the adapted fringe patterns are projected onto the object surface. The method requires prior

knowledge before measurement. Lyu *et al* [10] used an iterative algorithm to address the object with high dynamic range. The Fourier transform profilometry method is applied to build the correspondence relationship between the projection and object; then, an iterative method based on inversion algorithm is proposed to eliminate overexposure areas. Richard *et al* [11], presented a technique by illuminating the object multiple times from different directions and the unsaturated areas are extracted to form an image pattern for phase calculation. With this method, the object needs to be rotated many times and thus the method is not suitable for fast measurement. Hu *et al* [12] proposed to solve the problem by illuminating the object with multiple color light sources, and capturing the reflections by a set of cameras. This method is effective to eliminate the double bounce light for the measurement of shiny object. Chen *et al* [13], presented a method to deal with partial saturation in PSP technology. With this method, five phase-shift fringe patterns with the same intensity are projected and captured. The saturated points are detected based on intensity checking, which are removed and do not take part in the phase retrieval operation. In order to use PSP to obtain the phase map, for each pixel there must be three or more fringe patterns that are not saturated on the corresponding point. Therefore, this method is not effective for highly shinning surfaces due to the lack of unsaturated patterns. Instead of 5-step PSP, 7-step PSP was used by Hu *et al* [14], and the experiment shows that increasing the phase-shifting steps will improve the anti-saturation capability.

Recently, Zhang *et al* [15, 16] proposed to use multiple fringe patterns with different intensity levels to measure surfaces with a large range in its reflectivity. The projected fringe patterns are captured by a camera multiple times with different exposure time, resulting in a sequence of fringe images. The fringe patterns with the longest exposure time are the brightest and hence exhibit the largest areas of the saturation. With the decrease in exposure time the saturation areas also decrease and vanish, thus a set of images with decreasing saturation areas are obtained. In order to calculate the phase map, an unsaturated fringe images is synthesized on pixel-by-pixel basis by choosing the brightest but unsaturated corresponding pixel from the sequence of images and placing them in the same location with properly weighting. A similar method was proposed by Waddington *et al* [17]. Instead of changing exposure time of camera, the method presented in [17] employs different intensity levels of fringe patterns in the projector.

It is apparent that multiple fringe patterns are employed to address the saturation issue in the existing methods. However, with existing methods [15–17], only the data associated with brightest unsaturated images are utilized in the reconstruction, while all other unsaturated data (such as second or third brightest unsaturated images) are discarded, which is obviously a waste of information. In fact, the discarded unsaturated areas also carry the 3D information and can be used to improve the measurement accuracy. This paper presents a method making use of all the unsaturated image areas in order to achieve improved measurement accuracy.

This paper is organized as follows. Section 2 presents the principle of traditional multiple maximal intensity level method. In section 3, the proposed method is illustrated in detail and the combination model is given to reach high signal-to-noise ratio (SNR) result. In section 4, the experimental results are given to verify the effectiveness of the proposed algorithm. Section 5 concludes this paper.

2. Brief of existing methods

With PSP, a set of phase-shifted fringe patterns are generated by a digital projector, described as follows:

$$s_i(x,y) = a_0 + b_0 \cos\left(2\pi \frac{x}{\lambda_0} + \frac{2\pi i}{N}\right), \quad i = 1, \cdots, N \tag{1}$$

where $s_i(x,y)$ is the intensity of the projected fringe patterns, i is the index number, λ_0 is the spatial wavelength of the fringe pattern, a_0, b_0 and N denote the average intensity, intensity modulation and the number of steps for phase shifting respectively. These images are reflected by the surface of the object and captured by the camera as follows:

$$d_i^0(x,y) = a(x,y) + b(x,y)\cos\left(\varphi(x,y) + \frac{2\pi i}{N}\right), \quad i = 1, \cdots, N \tag{2}$$

where $a(x,y)$ denotes the ambient or background light captured by the camera. Note that in many practical applications such background light does exist when the measurement is not conducted in a dark room. $b(x,y)$ is the intensity modulation. $\varphi(x,y)$is the phase map of the captured fringe pattern, which is the modulation of the linear phase in equation (1) by the variance of the object shape, and hence carrying the information of the surface profile. The phase value can be obtained by equation (3):

$$\varphi(x,y) = \tan^{-1}\left[\sum_{i=1}^{N} d_i^0(x,y)\sin\left(\frac{2\pi i}{N}\right) \Big/ \sum_{i=1}^{N} d_i^0(x,y)\cos\left(\frac{2\pi i}{N}\right)\right]. \tag{3}$$

In order to avoid the sign ambiguity on the phase value, the double-argument atan2 function is employed when the algorithm is implemented. The above is the well-known phase-shifting algorithm for extracting the phase map of the reflected fringe patterns. This algorithm has a number of advantages, e.g. less influenced by the ambient light and reflectivity variations of the object surface. However, if the object surface contains shiny areas, the fringe patterns acquired may include saturation areas, and they cannot be correctly described by equation (2). In this case, equation (3) will not able to yield the correct phase map $\phi(x,y)$, and this will lead to significant error in the 3D reconstruction of the surface.

In order to remedy the above mentioned saturation issue, two separate pieces of work were carried out based on the same scenario [15, 17]. The idea was that, for each of phase-shifted fringe patterns $s_i(x,y)$, a set of the same pattern with different intensity level are generated by varying the camera exposure

time [15] or the projection intensity [17]. These patterns are projected onto the object and the reflections are captured by the camera as follows:

$$d_{i,j}(x,y) = p_j d_i(x,y), \qquad j = 1,2,\ldots,M \tag{4}$$

where M is the number of the intensity level;p_j reflects the influence of camera exposure time in [15]. or the projection intensity in [17]., which decreases with j. Note that $d_i(x,y)$ in equation (4) may not be the same at that in equation (2) due the influence of the saturation. $d_{i,1}(x,y)$ is the fringe patterns with the highest intensity and hence it has the largest saturated areas, and $d_{i,M}(x,y)$ is fringe patterns with the lowest intensity and containing no saturation areas. The techniques proposed in [15] and [17] are to construct a fringe pattern without having any saturation area. This is achieved on pixel-by-pixel basis by selecting the brightest but unsaturated corresponding pixels from the M patterns. In other words, the new fringe pattern is constructed by combining the following areas:

- The unsaturated areas on $d_{i,1}(x,y)$.
- The unsaturated areas on $d_{i,2}(x,y)$ excluding the unsaturated areas on $d_{i,1}(x,y)$.
- The unsaturated areas on $d_{i,3}(x,y)$ excluding the unsaturated areas on $d_{i,2}(x,y)$.
- …
- The unsaturated areas on $d_{i,M}(x,y)$ excluding the unsaturated areas on $d_{i,M-1}(x,y)$.

With such a method, a new fringe pattern without saturation can be obtained. However, the method is not efficient as for each of the fringe patterns in equation (4), only a small portion (area) is used, and the remaining areas, either saturated or unsaturated, are simply discarded (such as the second brightest intensity but unsaturated image). In fact, as the discarded areas also contain the 3D information of the surfaces, they can be used to improve the robustness and accuracy of the reconstruction.

3. The method proposed

As mentioned above, the performance of measurement can be improved if all the unsaturated areas in the acquired fringe patterns are utilized. Without losing of generality, we assume that the saturation occurs when the intensity exceeds T_s, and hence we introduce the following to describe the saturated and unsaturated areas on the image in equation (4):

$$P_{i,j}(x,y) = \begin{cases} 1, & d_{i,j}(x,y) < T_s \\ 0, & d_{i,j}(x,y) = T_s \end{cases}. \tag{5}$$

The above can be used as a mask to retrieve the unsaturated (or the saturated) areas of the relevant images. For example, $P_{i,3}(x,y)d_{i,3}(x,y)$ picks all the unsaturated area of $d_{i,3}(x,y)$ by setting the pixels on the saturated areas to zero. As the number and size of saturated areas decrease with j, we can assume that:

$$P_{i,1}(x,y) \subset P_{i,2}(x,y) \subset P_{i,3}(x,y) \cdots \subset P_{i,M}(x,y). \tag{6}$$

Based on the above we can build the following:

$$A_{i,j}(x,y) = \begin{cases} P_{i,1}(x,y), & when \quad j = 1 \\ \bar{P}_{i,j-1}(x,y)P_{i,j}(x,y), & when \quad j = 2,3,\ldots,M \end{cases} \tag{7}$$

where $\bar{P}_{i,j}(x,y) = 1 - P_{i,j}(x,y)$. Note that:

- $A_{i,1}(x,y) = P_{i,1}(x,y)$ is the mask to extract all unsaturated pixels on $d_{i,1}(x,y)$. The areas on all other images corresponding to this mask are all saturated. Hence, when this mask is applied to all other images, unsaturated pixels are always obtained.
- $A_{i,2}(x,y) = \bar{P}_{i,1}(x,y)P_{i,2}(x,y)$ gives the mask to extract the pixels that are saturated on $d_{i,1}(x,y)$ but unsaturated on all other images.
- $A_{i,j}(x,y) = \bar{P}_{i,j-1}(x,y)P_{i,j}(x,y)$ is the mask for the pixels that are saturated on $d_{i,1}(x,y)$, …, and $d_{i,m-1}(x,y)$ but unsaturated on all other images.
- $A_{i,M}(x,y) = \bar{P}_{i,M-1}(x,y)P_{i,M}(x,y)$ gives the mask for the pixels that are saturated on $d_{i,1}(x,y)$, …, $d_{i,M-1}(x,y)$ but only unsaturated on $d_{i,M}(x,y)$.

Now we propose to construct the fringe pattern based on the following:

- In the areas defined by $A_{i,1}(x,y)$, the corresponding areas of all the M image patterns are unsaturated, and hence they will all be utilized.
- In the areas defined by $A_{i,2}(x,y)$, the corresponding areas of $M-1$ image patterns $d_{i,j}(x,y)$ ($j = 2$, .,M) are unsaturated and employed.
- In the area defined by $A_{i,j}(x,y)$, the corresponding areas of $M-m+1$ image patterns $d_{i,j}(x,y)$ ($j = m$, .,M) are unsaturated and hence employed.
- In the area defined by $A_{i,M}(x,y)$, only the corresponding areas of $d_{i,M}(x,y)$ are unsaturated and utilized.

With the above, all the data associated with the unsaturated areas on all the images acquired are employed, and hence all information carried by them is utilized. Letting $U_i(x,y)$ denote the constructed fringe pattern, the areas masked by $A_{i,m}(x,y)$ should be constructed by the following:

$$U_i(x,y)A_{i,m}(x,y) = \sum_{j=m}^{M} k_{m,j} d_{i,j}(x,y)A_{i,m}(x,y) \tag{8}$$

where $k_{m,j}$ is a scaling factor, which should be selected in such a way to yield the maximal SNR for the area masked by $A_{i,m}(x,y)$. In order to determine $k_{m,j}$, we assume that all acquired fringe patterns contain additive random noise, i.e. $d_{i,j}(x,y) = p_j d_i(x,y) + n(x,y)$, and replacing it in equation (8) gives:

$$U_i(x,y)A_{i,m}(x,y) = \sum_{j=m}^{M} k_{m,j}\{p_j d_i(x,y) + n_j(x,y)\}A_{i,m}(x,y)$$

$$= \sum_{j=m}^{M} k_{m,j} p_j d_i(x,y) A_{i,m}(x,y) + \sum_{j=m}^{M} k_{m,j} n_j(x,y) A_{i,m}(x,y)$$
$$= d_i(x,y) A_{i,m}(x,y) \sum_{j=m}^{M} k_{m,j} p_j + A_{i,m}(x,y) \sum_{j=m}^{M} k_{m,j} n_j(x,y). \tag{9}$$

The first term in equation (9) corresponds to the synthesized pattern without noise, and the second term is the resulting noise component. Assuming the additive noise is of zero mean, variance σ^2 and independent with respect to j, the power of the noise component is:

$$[A_{i,m}(x,y)]^2 \sigma^2 \sum_{j=m}^{M} k_{m,j}^2. \tag{10}$$

Hence the SNR is given by:

$$SNR = \frac{[d_i(x,y) A_{i,m}(x,y)]^2 \left(\sum_{j=m}^{M} k_{m,j} p_j \right)^2}{[A_{i,m}(x,y)]^2 \sigma^2 \sum_{j=m}^{M} k_{m,j}^2}$$
$$= SNR_0 \frac{\left(\sum_{j=m}^{M} k_{m,j} p_j \right)^2}{\sum_{j=m}^{M} k_{m,j}^2} \tag{11}$$

where SNR_0 is the SNR associated with the fringe pattern $d_i(x,y)$ and additive noise $n(x,y)$.

Base on Cauchy inequality, the above reaches the maximum when $k_{m,j} = p_j t_m$, where t_m is a constant with respect to m. Therefore, equation (9) becomes

$$U_i(x,y) A_{i,m}(x,y)$$
$$= d_i(x,y) A_{i,m}(x,y) \sum_{j=m}^{M} t_m p_j^2 + n(x,y) A_{i,m}(x,y) \sum_{j=m}^{M} t_m p_j. \tag{12}$$

The above gives the area of reconstructed masked by $A_{i,m}(x,y)$. In order to construct a complete fringe pattern having the same shape as $d_i(x,y)$, the weight $\sum_{j=m}^{M} t_m p_j^2$ must be a constant with respect to j. Letting $\sum_{j=m}^{M} t_m p_j^2 = 1$, we have:

$$t_m = \frac{1}{(M-m+1) p_j^2} \tag{13}$$

and

$$k_{m,j} = P_j t_m = \frac{1}{(M-m+1) P_j} \tag{14}$$

and the SNR is given by:

$$SNR = SNR_0 \frac{\left(t_m \sum_{j=m}^{M} p_j^2 \right)^2}{t_m^2 \sum_{j=m}^{M} p_j^2} = SNR_0 \sum_{j=m}^{M} p_j^2. \tag{15}$$

Clearly, the SNR can be enhanced by carefully set of the weight.

With the above we can construct the fringe patterns as follows:

$$U_i(x,y) = \sum\nolimits_{m=1}^{M} U_i(x,y) A_{i,m}(x,y). \tag{16}$$

The above procedure can be summarized as follows:

Step 1: Acquisition of M fringe patterns with different intensity value, i.e. $d_{i,j}(x,y) = p_j d_i(x,y), \quad j = 1,2,\ldots,M$. Note that the first pattern ($j = 1$) should be as bright as possible capable of probing dark areas with the largest SNR ratio, and that the last pattern ($j = M$) should be the brightest one without saturation. M should be determined by the dynamic range of the reflectivity of the surface. The larger the range, the larger the value M.

Step 2: Obtain the mask functions $P_{i,m}(x,y), \quad m = 1, 2,\ldots,M$.

Step 3: Construct the mask functions $A_{i,m}(x,y), \quad m = 1, 2\ldots,M$ using equation (7).

Step 4: Use equation (8) to obtain areas of fringe pattern masked by $A_{i,m}(x,y)$. Note that the scaling factor $k_{m,j}$ should be computed by equation (14).

Step 5: Construct the fringe pattern $U_i(x,y)$ by equation (16).

Step 6: Repeat the above for all the N phase-shifted fringe patterns.

Step 7: Calculate the phase map using the reconstructed fringe patterns and reconstruct the 3D shape of the object surface.

4. Experiments

In order to show the effectiveness of the proposed method, we constructed a fringe projection profilometry (FPP) system using components of affordable price, including a DELL X1501 projector with the resolution of 1024 × 768 pixels, and a webcam GUKE HD91 (1920 × 1080 pixels). Compared with industrial cameras, the web camera is much cheaper in price but suffers from much higher noise in the captured image. The object to be measured is a plastic carton face shown in figure 1(a). Five step PSP is used to extract the phase map. When the object is projected by a fringe pattern with full intensity (the maximum intensity of the projector was set to 255), it is clear to see areas of saturation as shown in figure 1(b).

In order to apply the method proposed, eight levels of the fringe pattern intensity are produced and projected onto the object and the intensity decreases by 10% each time with their levels of intensity being 255, 229, 204, 178, 153, 127, 102,

Figure 1. The object used in the experiment. (a) The carton face object; (b) the captured fringe pattern of the object to be measured.

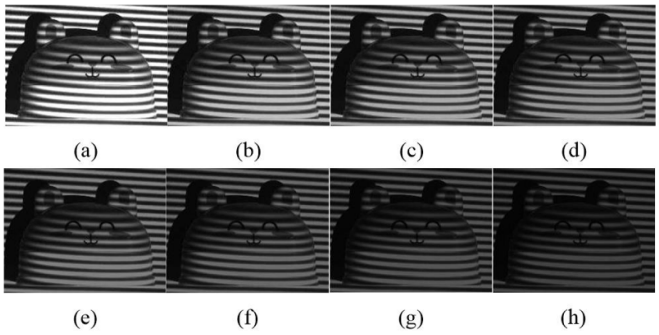

Figure 2. The captured fringe patterns with eight maximum intensity levels. (a)–(h): the captured fringe patterns of eight levels fringe intensity.

76. Note that when the minimum fringe pattern intensity is applied, there should be no saturation on the whole object. The captured fringe patterns are shown in figure 2. Clearly, saturation areas reduce with the decrease of the intensity. Note that the images with high intensity have the high SNR but suffer from large saturation areas. On the other hand, images with low intensity are characterized by small saturation, but they are disadvantageous by low SNR, making it hard to reconstruct the object.

Based on the fringe patterns acquired in figure 2, the masks identifying the saturation area can be obtained using equation (5) and are shown in figure 3. The threshold T_s is set to 255. For the specific pixel, when the intensity value equals to 255, the pixel is saturated. In figure 3, the black points are the saturation pixels and the white points present the unsaturation area. Figure 3(a) is the mask for figures 2(a) and 3(b) is the mask for the figure 2(b). It is also seen that, with the decrease of the maximum fringe intensity level, the saturation areas also reduce.

Based on method proposed, a new fringe pattern is constructed for each step of the PSP, as shown in figure 4(a). With the merged result, the wrapped phase value is retrieve and shown in figure 4(b).

Similarly to other PSP methods, phase unwrapping is always required to be applied to the wrapped phase to reconstruct the 3D information of the object. The results are shown in figures 5 and 6. Figure 5(a) is the front view of the reconstructed result. In order to see the detail of the reconstructed surface, one area on the object with zoom in view is given.

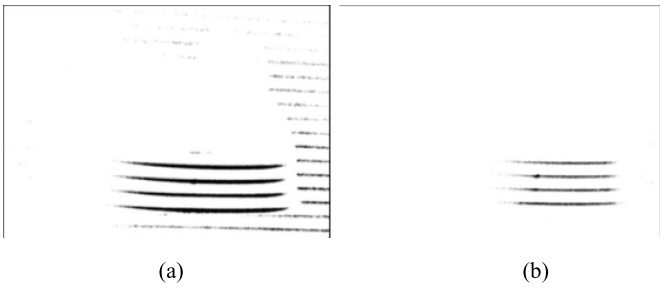

Figure 3. The mask identifying the saturation area. (a) The mask for figure 2(a); (b) the mask for figure 2(b).

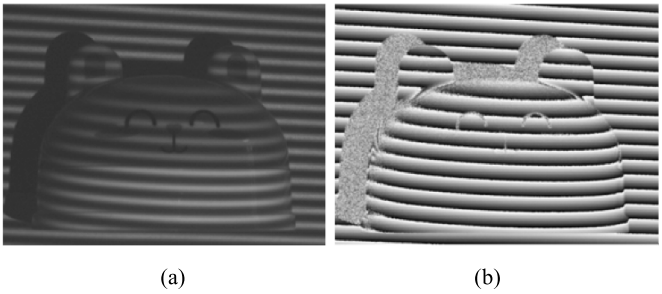

Figure 4. The merged fringe pattern and wrapped phase obtained by the proposed method. (a) The merged fringe pattern; (b) the wrapped phase value obtained by the proposed method.

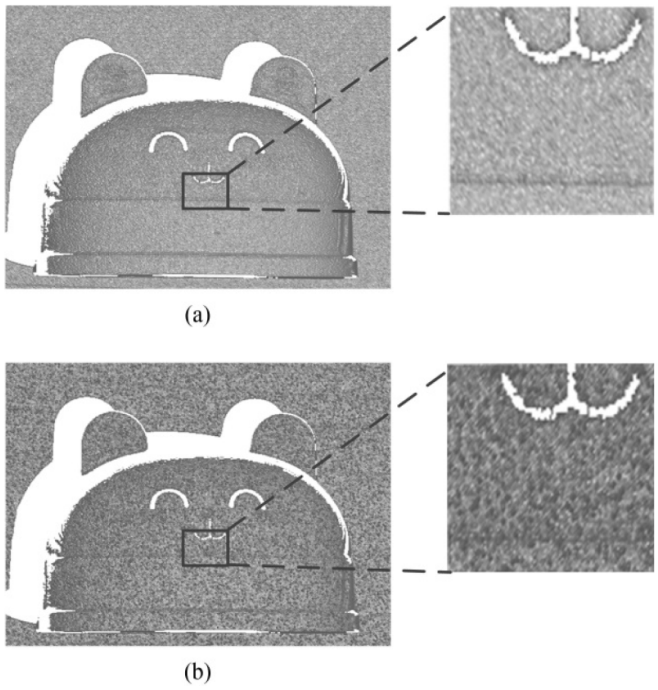

Figure 5. The reconstructed results. (a) The front view of the reconstructed result obtained by the proposed method; (b) the front view of the reconstructed result obtained by the [15].

Figure 6(a) is the mesh display of figures 5(a) and 6(c) is the cross line of the figure 6(a) when $x = 75$. It is apparent that all the areas including the saturated areas are reconstructed well and the surface is smooth.

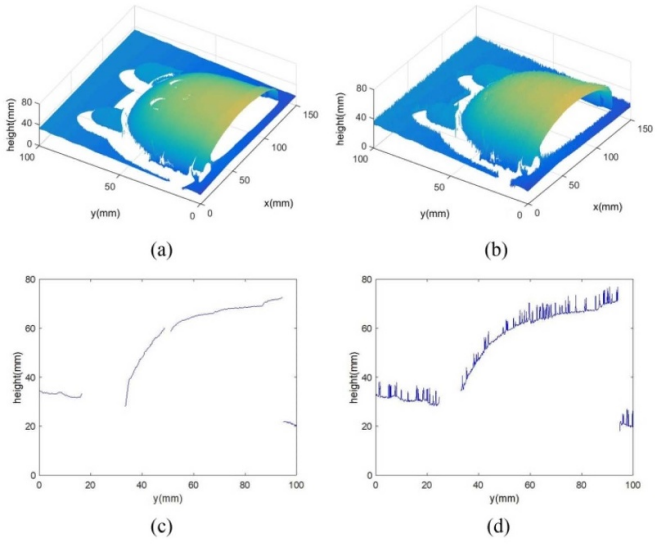

Figure 6. The comparison of the reconstruction results. (a) The mesh display of the result in figure 5(a); (b) the mesh display of the result in figure 5(b); (e) the cross line for figure 6(a) when $x = 75$; (f) the cross line for figure 6(b) when $x = 75$.

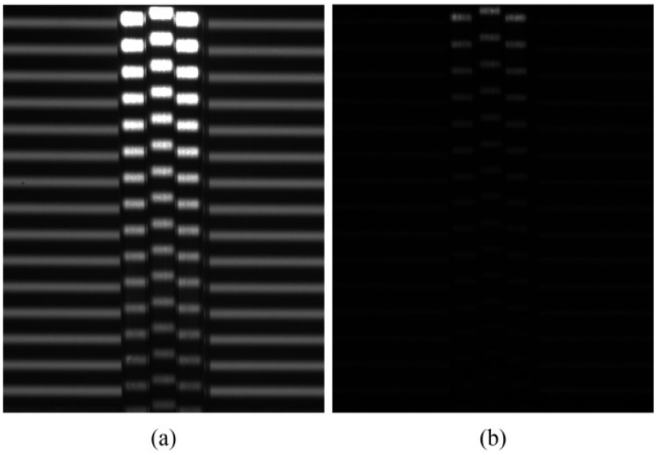

Figure 7. The captured fringe pattern image of metal object. (a) The fringe pattern image with the highest intensity; (b) the fringe pattern image with the lowest intensity.

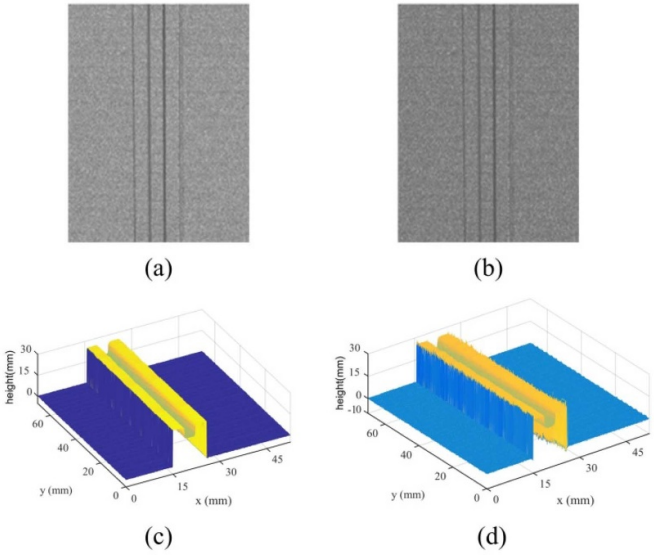

Figure 8. The reconstructed results of metal object. (a), (b) The front view of the reconstructed result obtained by the proposed method and [15]; (c), (d) The mesh display of figures 8(a) and (b).

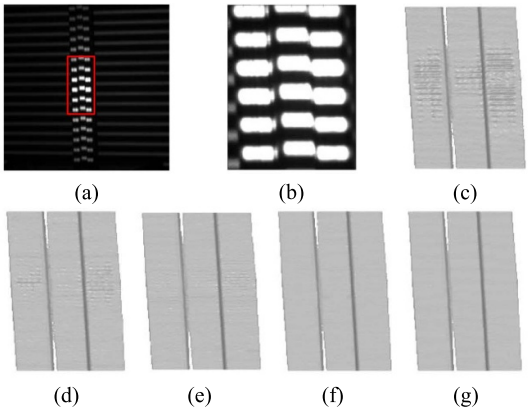

Figure 9. The reconstruction results with different phase shift step. (a) The captured fringe pattern with maximum intensity level; (b) the zoom in of the reconstructed part with saturation; (c)–(f) the reconstruction results with 6, 10, 14 and 18 steps PSP; (g) the reconstructed results of the proposed method with the intensity level of 250 and 170.

In order to verify the performance of the proposed method, the object is also reconstructed by the method in [15]. and the results are shown in figures 5(b), 6(b) and (d). Compared with the proposed method, the results by the method in [15]. contain significant errors. This is because they do not utilize all the unsaturation fringe patterns, and significant errors are introduced when the SNR is low. Note that the shadows are removed in the results shown in figures 5 and 6.

In the second experiment, a metal object with higher reflectivity is reconstructed. Eight intensity levels are employed. The captured fringe pattern with the highest intensity value and lowest intensity value is shown in figure 7. Compared with the image in figure 7(a), there is no saturation in figure 7(b).

The reconstructed results of the metal object are shown in figure 8. The proposed method improved the reconstruction accuracy significantly.

It should be pointed out that the errors caused by the saturation can also be reduced or eliminated by traditional PSP with large number of steps of phase shift. In order to compare the proposed method and the traditional PSP with large number of steps, we carried out experiment on the same object as shown in figure 9 using the traditional PSP with its steps increasing from 6 to 40. The captured fringe pattern is given in figure 9(a). The region with of saturation is magnified in figure 9(b).

Figures 9(c)–(f) present the reconstruction result with 6, 10, 14 and 18 step-PSP respectively. Significant error happens in the saturation pixels when the phase step is less than 18. It can be seen that with the increment of the steps, the area of the

saturation errors are reduced. When the number of the phase step is more than 18, the saturation influence is removed.

Then, the proposed method is applied to the same object. We found that two intensity levels are enough to avoid the saturation. The first intensity level is set to be 250 to obtain the maximum SNR of the unsaturation part in figure 9(b) and then decreased to 170 to avoid the saturation for other pixels in figure 9(b). The reconstructed result is shown in figure 9(g). It is apparent that the saturation errors are eliminated successfully.

As shown by experiment, the traditional PSP needs 18 steps, while the proposed method only requires 10 fringe patterns. Therefore, although the saturation error can also be alleviated by increasing the steps of the traditional PSP, the total number of fringe patterns required is higher than proposed method. This is because, in contrast to the traditional PSP where all fringe patterns have the same intensity and thus influenced by saturation, the proposed method only make use of the unsaturated component of the fringe patterns, and thus less impacted by the distortion error of the patterns.

In order to evaluate the anti-noise performance of the proposed method, we also calculated the RMS (root mean square) errors for the reconstruction results given in figures 5 and 8. With the proposed method, the RMS error with respect to figure 5(a) is 0.068 mm, and it is 11.07 mm for the results in figure 5(b). With the metal object, the RMS error for the result in figure 8(a) is 0.071 mm and 9.58 mm for the result in figure 8(b). Hence, the proposed method can significantly improve the measurement accuracy under low SNR.

The above experiments are implemented by the Matlab software, the computer includes Intel i7-7700 (2.81 GHz) processor and 16 GB RAM. The calculation time for the first experiment and second experiment is 10.8 s and 9.2 s respectively. The efficiency can be increased by the C++ coding and parallel computing in GPU.

Please note that the required frame number of the proposed method is $M \times N$. When the object has no saturation, only one intensity level ($M = 1$) is enough to reconstruct the object. In the other hand, when the object has saturation, M intensity levels are employed to remove the saturation influence, the frame number will be $M \times N$. The number of the intensity level depends on how complex of the object reflectivity.

5. Conclusion

This paper presents a method to address the saturation issue for the objects with a dynamic range of reflectivity variation. The proposed method utilizes all the unsaturation images thus is more effective for measuring the shiny surfaces by FPP with low-cost cameras. Comparing to existing methods only using the highest intensity of pixels for compositing image, the proposed method is able to significantly improve the measurement accuracy. It should be pointed out that the proposed method only works for the cases where unsaturated reflection can be obtained by reducing the intensity of projection. For the objects with very shinny surfaces, we may not be able to acquire a saturation-free fringe pattern, and in this case, the propose method will not work.

Acknowledgments

This research was supported by the National Natural Science Foundation of China (61705060).

ORCID iD

Lei Lu https://orcid.org/0000-0002-3050-6542

References

[1] Gorthi S and Rastogi P 2010 Fringe projection techniques: whither we are? *Opt. Lasers Eng.* **48** 133–40
[2] Lu L, Xi J, Yu Y and Guo Q 2013 New approach to improve the accuracy of 3-D shape measurement of moving object using phase shifting profilometry *Opt. Express* **21** 30610–22
[3] Lu L, Ding Y, Luan Y, Yin Y, Liu Q and Xi J 2017 Automated approach for the surface profile measurement of moving objects based on PSP *Opt. Express* **25** 32120–31
[4] Zhang S, Weide D and Oliver J 2010 Superfast phase-shifting method for 3-D shape measurement *Opt. Express* **18** 9684–9
[5] Feng S, Zhang L, Zuo C, Tao T, Chen Q and Gu G 2018 High dynamic range 3D measurements with fringe projection profilometry: a review *Meas. Sci. Technol.* **29** 122001
[6] Zheng Y, Wang Y, Suresh V and Li B 2019 Real-time high-dynamic-range fringe acquisition for 3D shape measurement with a RGB camera *Meas. Sci. Technol.* **30** 075202
[7] Wang Y, Zhang J and Luo B 2018 High dynamic range 3D measurement based on spectral modulation and hyperspectral imaging *Opt. Express* **26** 34442–50
[8] Jiang H, Zhao H and Li X 2012 High dynamic range fringe acquisition: a novel 3-d scanning technique for high-reflective surfaces *Opt. Lasers Eng.* **50** 1484–93
[9] Chen C, Gao N, Wang X and Zhang Z 2018 Adaptive projection intensity adjustment for avoiding saturation in three-dimensional shape measurement *Opt. Commun.* **410** 694–702
[10] Lyu C, Bai Y, Yang J, Qi H and Ma J 2020 An iterative high dynamic range image processing approach adapted to overexposure 3D scene *Opt. Lasers Eng.* **124** 105831
[11] Kowarschik R, Kuehmstedt P, Gerber J, Schreiber W and Notni G 2000 Adaptive optical three-dimensional measurement with structured light *Opt. Eng.* **39** 150 –8
[12] Hu Q, Harding K, Du X and Hamilton D 2005 Shiny parts measurement using color separation *Proc. SPIE* **6000** 60000D
[13] Chen Y, He Y and Hu E 2008 Phase deviation analysis and phase retrieval for partial intensity saturation in phase-shifting projected fringe profilometry *Opt. Commun.* **281** 3087–90
[14] Hu E, He Y and Wu W 2010 Further study of the phase-recovering algorithm for saturated fringe patterns with a larger saturation coefficient in the projection grating phase-shifting profilometry *Optik* **121** 1290–4
[15] Zhang S and Yau S 2009 High dynamic range scanning technique *Opt. Eng.* **48** 033604
[16] Zhang S 2020 Rapid and automatic optimal exposure control for digital fringe projection technique *Opt. Lasers Eng.* **128** 10629
[17] Waddington C and Kofman J 2014 Modified sinusoidal fringe-pattern projection for variable illuminance in phase-shifting three-dimensional surface-shape metrology *Opt. Eng.* **53** 084109